MedChemComm

RSC Publishing

CONCISE ARTICLE

View Article Online
View Journal | View Issue

Cite this: *Med. Chem. Commun.*, 2013, **4**, 456

Identification of pyrazolo-pyrimidinones as GHS-R1a antagonists and inverse agonists for the treatment of obesity†

William McCoull,*[a] Peter Barton,[a] Anders Broo,[b] Alastair J. H. Brown,[a] David S. Clarke,[a] Gareth Coope,[a] Robert D. M. Davies,[a] Alexander G. Dossetter,[a] Elizabeth E. Kelly,[a] Laurent Knerr,[b] Philip MacFaul,[a] Jane L. Holmes,[a] Nathaniel Martin,[a] Jane E. Moore,[a] David Morgan,[a] Claire Newton,[a] Krister Österlund,[b] Graeme R. Robb,[a] Eleanor Rosevere,[a] Nidhal Selmi,[b] Stephen Stokes,[a] Tor S. Svensson,[b] Victoria B. K. Ullah[b] and Emma J. Williams[a]

Received 9th November 2012
Accepted 15th December 2012

DOI: 10.1039/c2md20340e

www.rsc.org/medchemcomm

A pyrazolo-pyrimidinone based series of growth hormone secretagogue receptor type 1a (GHS-R1a) antagonists and inverse agonists were identified using a scaffold hop from known quinazolinone GHS-R1a modulators. Lipophilicity was reduced to decrease hERG activity while maintaining GHS-R1a affinity. SAR exploration of a piperidine substituent was used to identify small cyclic groups as a functional switch from partial agonists to neutral antagonists and inverse agonists. A tool compound was identified which had good overall properties and sufficient oral plasma and CNS exposure to demonstrate reduced food intake in mice through a mechanism involving GHS-R1a.

Introduction

Ghrelin, a 28 amino acid acylated peptide hormone is the endogenous ligand of the growth hormone secretagogue receptor type 1a (GHS-R1a).[1] The major physiological role of ghrelin appears to be in the control of food intake and energy homeostasis.[2] Energy intake and body weight are tightly regulated at a remarkably consistent set-point by control systems in the hypothalamus.[3] While the role of ghrelin in this system is still not fully understood, it is clear that acylated ghrelin is released from specialized mucosal cells in response to hunger cues. This results in a peak of plasma ghrelin levels before meal initiation[4] that is consistent with a role in meal initiation. In addition, ghrelin infusion in both rodents and humans increases appetite and food intake.[5] Consequently, peripheral and CNS penetrant ghrelin receptor antagonists have been proposed as potential therapeutic agents for the treatment of obesity[6–10] and type II diabetes.[11] Furthermore, due to the apparent constitutive activity of the ghrelin receptor demonstrated in recombinant cell systems and in rodents, we believe that inverse agonists may have additional benefit over 'neutral' antagonists in lowering the set-point for hunger between meals.[12]

We are interested in identifying GHS-R1a antagonists and inverse agonists for the treatment of obesity. Several structurally diverse antagonists have been reported[9,10,13–22] and some have been shown to act as inverse agonists.[19,22] We were attracted to a quinazolinone series reported to have demonstrated CNS exposure (Fig. 1).[13,14] Quinazolinone **1** typified this structural class showing high affinity (IC_{50} = 0.0001 μM) in a ^{125}I-ghrelin displacement assay, but with numerous undesirable properties. Activity at the hERG encoded potassium channel[23] (IC_{50} = 8.7 μM), modest aqueous solubility at pH 7.4 (45 μM), and activity against cytochrome P450 enzymes (CYP3A4 inhibition IC_{50} = 0.68 μM) are all consistent with high measured lipophilicity (log $D_{7.4}$ > 4.3). Another quinazolinone **2** (YIL-870) with lower affinity (IC_{50} = 0.052 μM) was reported to significantly reduce body weight in DIO mice.[14] However, we have determined that the effects of this specific compound on body weight are independent of GHS-R1a (see ESI†). Both **1** and **2** do not demonstrate pharmacological properties consistent with inverse agonism as measured in a Tango™ functional assay thus are likely to represent neutral antagonists or weak partial agonists. We anticipated that many of these undesirable properties could be improved upon by reducing lipophilicity and that the functional activity could be tuned to give an inverse agonist through SAR exploration. Consequently we planned to use a scaffold hopping approach, switching the bicyclic core, then modify the two aryl substituents to improve ligand

[a]*Cardiovascular and Gastrointestinal Innovative Medicines Unit, AstraZeneca, Alderley Park, Macclesfield, Cheshire, SK10 4TG, UK. E-mail: william.mccoull@astrazeneca.com; Tel: +44 (0) 1625 519444*

[b]*Cardiovascular & Gastrointestinal Innovative Medicines Unit, AstraZeneca, Pepparedsleden 1, 431 83, Mölndal, Sweden*

† Electronic supplementary information (ESI) available: Synthetic details for the preparation of compounds and protocols for biological and physicochemical measurements. See DOI: 10.1039/c2md20340e

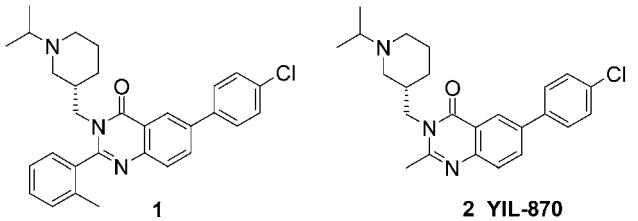

Fig. 1 GHS-R1a modulators from quinazolinone series.[13,14]

lipophilicity efficiency (LLE).[24] Since the chiral piperidine is important to receptor binding we planned to keep this ring but target the alkyl sidechain on the piperidine nitrogen to probe SAR for inverse agonism while also reducing basicity to minimise likelihood of off-target pharmacology for a CNS agent.[24] We reasoned that the combination of these gross structural changes would increase the likelihood of avoiding the off-target effects associated with **2**. In this paper we describe the reduction to practice of this strategy to afford potent pyrazolo-pyrimidinone based GHS-R1a antagonists and inverse agonists, providing a tool compound with oral plasma and CNS exposure suitable for evaluation in preclinical efficacy models.

Results and discussion

Thieno-pyrimidinone and thiazolo-pyrimidinone synthesis is exemplified in Scheme 1. Aminoester **5** was obtained from **3** using Liebeskind–Srogl coupling.[25] Subsequent condensation with the imidoyl chloride generated from benzamide **6** afforded amidines that were directly ring closed using $TiCl_4$ (ref. 26) and microwave heating, to obtain **7** and **8**.

Intermediate 2-substituted 4-aminopyrazoles **11** were prepared in three steps from nitro pyrazole acid **9** (Scheme 2). Esterification using continuous flow chemistry minimised handling large amounts of potentially explosive nitro pyrazole. Then Chan–Lam couplings[27] followed by reduction of the nitro group efficiently generated a diverse set of 2-aryl pyrazoles **11**.

Synthetic routes to allow diversity at three positions of the pyrazolo-pyrimidinone were developed as shown in Scheme 3.

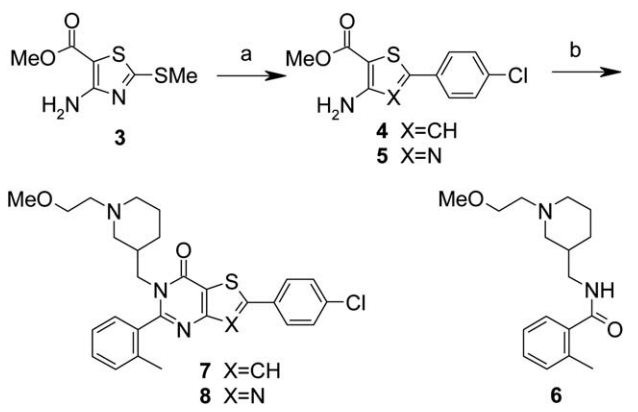

Scheme 1 *Reagents and conditions*: (a) 4-Cl-phenylboronic acid, copper(I) salicylate, $Pd(PPh_3)_4$, THF, 50 °C, 70 h, 69%; (b) (i) **6**, $POCl_3$, DCE, 16 h, 85 °C, (ii) $TiCl_4$, DCE, 170 °C, μW, 10 min, 60% (**7**) or **6**, $TiCl_4$, DCE, 170 °C, μW, 40 min, 16% (**8**).

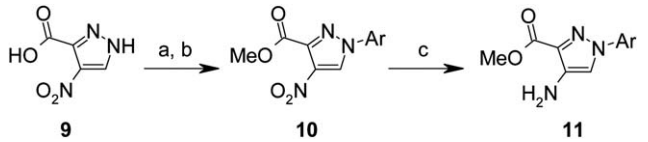

Scheme 2 *Reagents and conditions*: (a) MeOH, H_2SO_4, 81%; (b) $ArB(OH)_2$, $Cu(OAc)_2$, py, air, DCM, 22–81%; (c) Pd/C, H_2 or Fe, HCl, 23–87%.

Acylation of the requisite aminopyrazole **11** with 2-methylnicotinic acid was carried out under standard amide coupling conditions and the resulting amide **12** chlorinated with phosphorous pentachloride. Amidine formation with (*R*)-*tert*-butyl 3-(aminomethyl)piperidine-1-carboxylate and cyclisation under basic conditions gave the pyrazolo-pyrimidinone core in **13**. The intermediate imidoyl chloride was unstable and partly rearranged to an acyl chloride leading to the formation of some bis-amide side product **15**. Removal of the Boc protecting group and either alkylation or reductive amination allowed for pyrazolo-pyrimidinones **14** to be synthesized with a variety of substituents on the piperidine nitrogen.

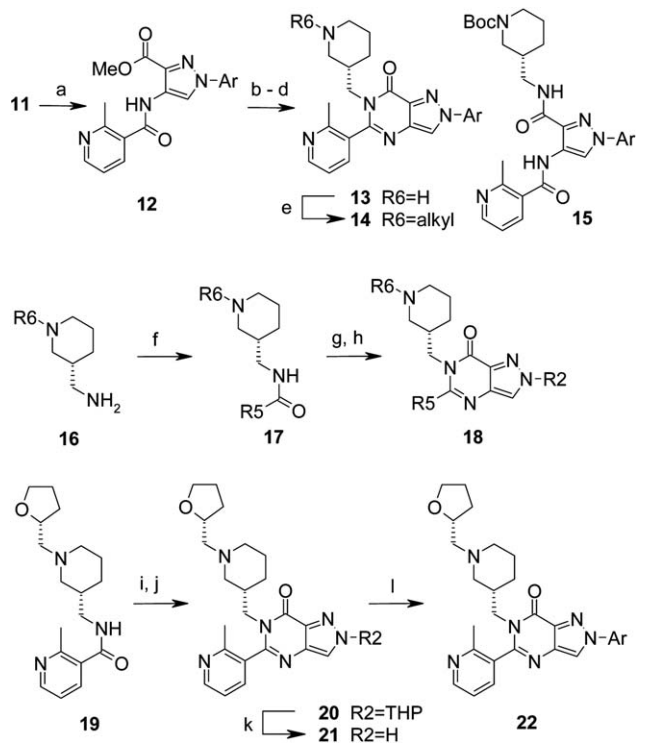

Scheme 3 *Reagents and conditions*: (a) 2-Me-nicotinic acid, HATU or HBTU, DIPEA, DCM or DMF, r.t, 48 h, 71–79%; (b) PCl_5, toluene, 110 °C, 4–6 h then (*R*)-*tert*-butyl 3-(aminomethyl)piperidine-1-carboxylate, DIPEA, DCE; (c) K_2CO_3, DMF, 130 °C, 45 min, 19–45% (2 steps); (d) 4 M HCl in 1,4-dioxane, r.t, 16 h, 80–100%; (e) $Na(AcO)_3BH$, DCE, AcOH, ketone or aldehyde, 34–65%; or R6–I/Br, K_2CO_3, DMF, or dioxane, 80–100 °C, 23–66%; or R6–OTs, MeCN or DMF, 90–130 °C, 8–44%; (f) R5–COCl, NEt_3, DCM, 81%; (g) PS-PPh_3, CCl_4, NEt_3 then aminopyrazole **11**, DIPEA or $POCl_3$, DCE, 16 h, 85 °C; (h) K_2CO_3, DMF, 100 °C, 16 h or $TiCl_4$, DCE, 150 °C, 10 min, 29–73% (2 steps); (i) PS-PPh_3, CCl_4, NEt_3 then 4-amino-5-ethoxycarbonyl-2-tetrahydropyranyl-pyrazole; (j) K_2CO_3, DMF, 100 °C, 16 h, 54% (2 steps); (k) 2 M HCl, r.t, 16 h, 92%; (l) $Cu(OAc)_2$, py, DCM, air, 22–30%.

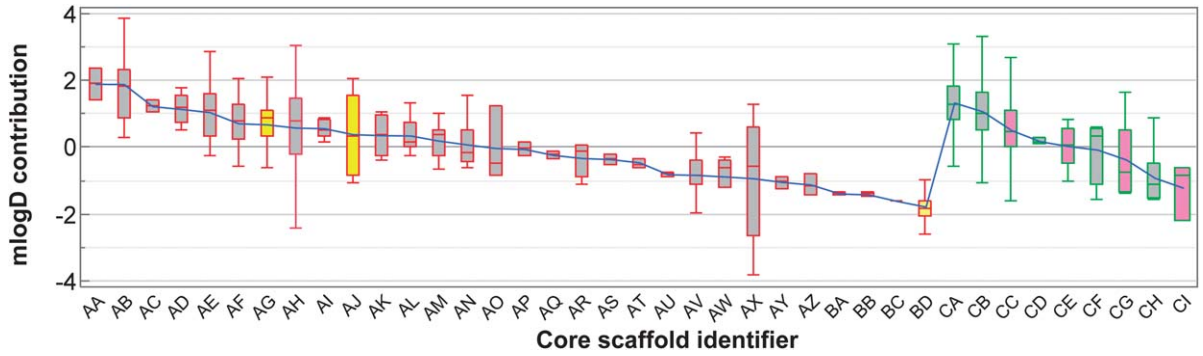

Fig. 2 Box and whisker plot showing predicted log *D* of bicyclic cores considered for scaffold hop. Boxes indicate 25th, 50th (median) and 75th percentiles. Whiskers show full data range, excluding outliers. Blue line connects the mean log *D* for each core. A yellow background indicates cores that were synthesised in this work (AG, AJ, BD). A pink background indicates quinazolinone and related compounds, previously reported (CC, CE, CG, CI). 5,6-Bicycles start A or B, 6,6-bicycles start with C. Full core names and data detail in ESI.†

Alternatively, acylation of an 3-aminomethyl piperidine **16** and chlorination[28] of the resulting amide **17** under mild conditions gave an intermediate imidoyl chloride which could be smoothly condensed with a 2-substituted 4-aminopyrazoles **11**. Cyclisation of the resulting amidine gave the pyrazolo-pyrimidinone core in **18**, avoiding the bis-amide side product.

To allow for late-stage variation of the aryl substituent on the pyrazole a tetrahydropyranyl (THP)-protected pyrazole was employed. The pyrazolo-pyrimidinone core was assembled with THP at R2 (**20**). Then THP-deprotection gave **21** followed by Chan–Lam coupling to give the desired arylated compounds **22** (along with their *N*-1 regioisomers).

Initial chemistry efforts were focused on replacing the quinazolinone with a less lipophilic bicyclic core. Our design strategy involved identifying potential bicyclic systems that existed in the AstraZeneca compound collection with measured log $D_{7.4}$ (*m*log *D*). Substructure log *D* values were calculated using ACDlog *D* (pH 7.4) for each substituent, the sum of which was subtracted from the *m*log *D* to obtain a predicted log *D* for the core. Averaging over several compounds is a method to minimise the effect of noise due to errors in both the calculated and measured log *D* components.[29] This is a more reliable method of identifying the contribution of the core in a fully elaborated molecule rather than simply using calculated log *D* of the unsubstituted core. Potential cores could then be vetted for likelihood of lowering log *D* and since we restricted ourselves to AstraZeneca compounds, synthetic routes were also likely to exist. Fig. 2 shows that the quinazolinone core (CC) is one of the more lipophilic cores and several more hydrophilic opportunities existed *e.g.* thiazolo-pyrimidinones (AJ) and pyrazolo-pyrimidinones (BD) – the core with predicted lowest log *D*. Thieno-pyrimidinones (AG) have similar predicted log *D* to quinazolinones and several aza-modified quinazolinone cores (CE, CG and CI) predict lower log *D* as has been reported by others.[18]

Three cores were prepared and compared with quinazolinone **1** (Table 1). Thienopyrimidinone **23** was initially selected to confirm changing to a five-membered ring was tolerated, with some reduction in potency in light of enantiopure **1** being compared with racemates. Pyrazolo-pyrimidinone **24** was shown to maintain affinity. It is difficult to obtain accurate log $D_{7.4}$ data on high lipophilicity compounds using a shake-flask

Table 1 GHS-R1a binding affinity, lipophilicity, LLE, hERG and pK_a for selected bicyclic core variations

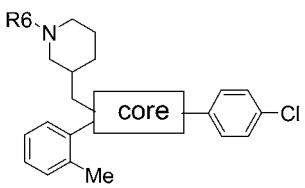

Cpd	Core (identifier)	R6	GHS-R1a IC_{50}[a] (μM)	HPLC log D[c]	log $D_{7.4}$	LLE[d]	hERG IC_{50} (μM)	pK_a
1[b]	Quinazolinone (CC)	i-Pr	0.00012	5.0	>4.3	4.9	8.7	—
23	Thieno-pyrimidinone (AG)	i-Pr	0.0015	4.8	—	4.0	2.1	—
24	Pyrazolo-pyrimidinone (BD)	i-Pr	0.00028	3.2	—	6.4	3.5	10.0
7	Thieno-pyrimidinone (AG)	CH_2CH_2OMe	0.016	5.6	>4.3	2.2	2.1	8.5
8	Thiazolo-pyrimidinone (AJ)	CH_2CH_2OMe	0.059	5.1	3.5	2.1	3.7	9.2
25	Pyrazolo-pyrimidinone (BD)	CH_2CH_2OMe	0.0011	3.7	3.3	5.3	2.5	8.5

[a] Mean values of at least two experiments. [b] (3*S*)-Piperidine rather than racemate. [c] Measured using chromatographic method.[30] [d] Using HPLC log *D*.

method, thus an alternative measure of log *D* based on chromatography[30] was used. This HPLC log *D* data indicated that pyrazolo-pyrimidinone **24** demonstrated significant lipophilicity decrease over both quinazolinone **1** and thieno-pyrimidinone **23** (3.1 for **24**, compared to 5.0 for **1** and 4.8 for **23**). High basicity is expected from the *N*-iso-propyl piperidine which, coupled with high lipophilicity is associated with an increased risk of promiscuity.[24] Thus we commonly used ether containing groups such as methoxyethyl (compounds **7**, **8**, **25**) to lower pK_a. Some reduction in potency resulted but pyrazolo-pyrimidinone **25** again showed lower lipophilicity than thieno-pyrimidinone **7** or thiazolo-pyrimidinone **8**. Use of HPLC log *D* to calculate LLE identifies pyrazolo-pyrimidinones as superior to the other cores. Activity against the hERG encoded potassium channel persisted in the low micromolar range for all these compounds.

We decided to focus on the pyrazolo-pyrimidinone core but realised that further lipophilicity reduction was required to improve overall properties such as hERG activity (Table 2). The 4-Cl-phenyl group could be varied to reduce log $D_{7.4}$ while still maintaining nanomolar binding affinity in many cases (compounds **26–36**). Incorporating pyridine into the R5-*ortho* tolyl group gave a further log $D_{7.4}$ reduction while maintaining potency as in **34** compared to **30**. Activity against hERG was now consistently greater than 10 μM, irrespective of the basicity. As found previously, reducing the piperidine pK_a from 10 to 8.5 was well tolerated but ablation of basicity was not tolerated as in oxetane **33**. Removal of the R2 aryl group or conversion to saturated substituents such as c-hexyl **36** resulted in significant reduction of potency. For the next phase of optimisation, R5 = 2-methyl-3-pyridyl and R2 = 3-methoxyphenyl was selected as the optimal substituents based on ease of synthesis and overall properties. For example, **34** exhibited aqueous solubility of >2700 μM, low plasma protein binding (63% free and 57% free in human and mouse respectively), no significant activity

Table 2 GHS-R1a binding potency, hERG activity, log $D_{7.4}$, LLE and pK_a for selected compounds

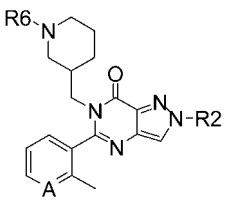

Cpd	A	R6	R2	GHS-R1a IC_{50}[a] (μM)	log $D_{7.4}$	LLE	hERG IC_{50} (μM)	pK_a
24	CH	i-Pr	4-Cl-Ph	0.00028	—	—	3.5	10.0
26	CH	i-Pr	4-F-Ph	0.0011	2.3	6.7	>10	10.0
27	CH	i-Pr	4-CN-Ph	0.012			>8.3	10.0
28	CH	i-Pr	4-MeO-Ph	0.0073	2.4	5.7	11	10.0
29	CH	i-Pr	3-Cl-Ph	0.0016	3	5.8	10	9.8
30	CH	i-Pr	3-MeO-Ph	0.0018	2.5	6.3	15	10.0
31	CH	i-Pr	3-CN-Ph	0.032	1.8	5.7	22	9.9
32	N	CH_2CH_2OMe	4-CN-Ph	0.044	1.1	6.3	21	8.5
33	N	Oxetan-3-yl	4-CN-Ph	4	1.2	4.2		6.4
34[b]	N	i-Pr	3-MeO-Ph	0.0017	1.3	7.5	47	9.7
35[b]	N	CH_2CH_2OMe	3-MeO-Ph	0.0061	1.3	6.9	43	8.4
36[b]	N	CH_2CH_2OMe	*c*-Hex	0.37	1.4	5	>100	—

[a] Mean values of at least two experiments. [b] (3*S*)-Piperidine rather than racemate.

Table 3 GHS-R1a binding affinity, and functional effect for selected compounds varying R6

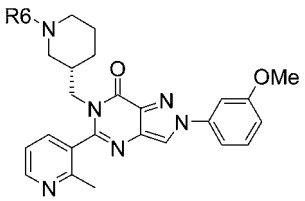

Cpd	R6	GHS-R1a IC_{50}[a] (μM)	Agonist effect[a,b] (%)	Inverse agonist effect[a,b] (%)
35	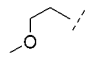	0.0061	78	<10
37	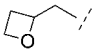	0.023	21	<10
38	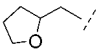	0.0076	<10	23
39	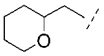	0.12	<10	16
40	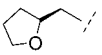	0.015	11	<10
41	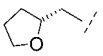	0.0051	<10	55
42	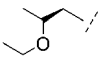	0.005	70	<10
43	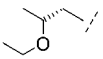	0.04	55	<10
44	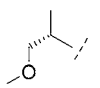	0.0017	74	<10
45	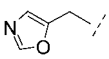	0.12	53	<10
46	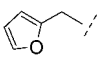	0.0027	64	<10
47	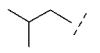	0.0057	<10	<10
48	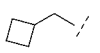	0.0016	11	10
49	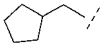	0.012	<10	59
50	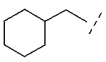	0.2	14	<10
51	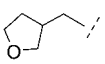	0.06	45	<10

[a] Mean values of at least two experiments. [b] Maximum% activation, maximum concentration = 10 μM.

against cytochrome P450 enzymes CYP1A2, CYP2C9, CYP2C19, CYP2D6 and CYP3A4 (all >30 μM), in addition to high LLE of 7.5. However, **34** exhibited full agonism in a Tango functional assay with EC_{50} = 0.0013 μM (92% maximal agonist effect) and this undesired functional effect was addressed next.

Our attempts to modulate functional activity focused on the piperidine substituent, based on functional modulation reported in the quinazolinone work.[13] In our pyrazolo-pyrimidinones we also found this substituent to influence functional activity but with very specific SAR as shown in Table 3. Introduction of cyclic substituents reduced the agonist response as in ethers **37–39** with the 5-membered ring exhibiting potent binding affinity and partial inverse agonism. The activity was found to be dependent on stereochemistry with the (*S*)-tetrahydrofuran **40** exhibiting neutral antagonism but (*R*)-tetrahydrofuran **41** exhibiting inverse agonism. Branched acyclic analogues **42–44** are all partial agonists, as are hetaryl analogues exemplified by **45** and **46**. Alkyl analogues **47–50** demonstrated similar trend in functional activity with the 4 and 6-membered rings being neutral antagonists and the c-pentyl analogue **49** being an inverse agonist. Interestingly, the regioisomeric tetrahydrofuran **51** is a partial agonist, again highlighting the very specific nature of functional SAR in this series. While we do not have an full understanding of the interaction of these compounds with the receptor, a binding pocket has been proposed which can lead to the opposite efficacy and our results are consistent with finding.[31] Having identified the (*R*)-tetrahydrofuran as a functional switch, we performed a further SAR iteration to identify an inverse agonist with CNS exposure suitable as a tool for preclinical efficacy experiments. Gratifyingly, the (*R*)-tetrahydrofuran maintained inverse agonism when the R2-aryl or R5-pyridyl groups were modified (Table 4). Smaller groups at R5, for example methyl (**52**) and iso-butyl (**53**) did maintain neutral antagonism or inverse agonism but with a significant reduction in affinity thus were not progressed. Variations at R2-aryl substitution maintained inverse agonism with some variation in maximal response but also a marked SAR for binding affinity depending on the ether substituent. 4-Methoxy **55** has 4-fold greater affinity than unsubstituted **54**. Moving methoxy from 4- to 3-position as in **41** increased affinity 10-fold further and the larger 3-ethoxy **56** gave 5-fold more affinity increase. Di-F-methyl ether **59** exhibited the largest inverse agonist response. The larger ethers have higher lipophilicity resulting in increased hERG activity, higher metabolic clearance and only **56** has improved LLE over **41**. Since we were interested in a CNS penetrant compound, a hybrid ligand efficiency parameter (LE fub) incorporating potency and free fraction in brain,[32] as an indicator of receptor occupancy[33] was monitored throughout the optimisation process. Our aim was to at least match the value of antagonist **1** (LE fub = 6.8) with our pyrazolo-pyrimidinone inverse agonist tool. Consequently **41** was judged to have the most attractive profile and confirmed to have suitable plasma and CNS exposure following oral dosing (Table 5).

In a free feeding test, compound **41** (20 mg per kg po) was administered to ad libitum fed GHS-R1a null (KO) and wild-type (WT) mice and food intake measured at two-hourly intervals (Fig. 3a). Over the first 2 h time interval food intake in WT mice is reduced by 68% but with no significant change in KO mice. The difference in food intake at 2 h between WT and KO mice treated with vehicle is consistent with what we observe in other studies using this model.

Similar exposure levels of **41** were observed in KO and WT mice and free exposure levels in brain were sustained above the binding affinity over the first 2 h time interval (Fig. 3b). This result is consistent with the feeding being blocked by inverse agonist **41** through a mechanism involving GHS-R1a. The effect

Table 4 GHS-R1a binding affinity, functional effect, hERG activity, log $D_{7.4}$, LLE, human liver microsome (HLM) metabolism and LE fub for selected compounds

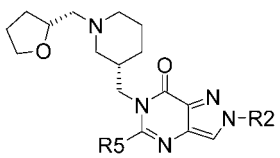

Cpd	R5	R2	GHS-R1a IC_{50}[a] (μM)	Agonist effect[a,b] (%)	Inverse agonist effect[a,b] (%)	hERG IC_{50} (μM)	log $D_{7.4}$	LLE	HLM Cl_{int} (μl min^{-1} mg^{-1})	LE fub[c]
41	2-Me-3-pyridyl	3-MeO-Ph	0.0051	<10	55	44	2	6.3	17	7.2
52	Me	3-MeO-Ph	0.98	28	<10	2.9	1.9	4.1	16	
53	i-Bu	3-MeO-Ph	0.5	<10	36	3.2	3.1	3.2	60	4.7
54	2-Me-3-pyridyl	Ph	0.19	<10	10	12	1.7	5	15	6
55	2-Me-3-pyridyl	4-MeO-Ph	0.052	<10	58	4.1	1.9	5.4	21	6.3
56	2-Me-3-pyridyl	3-EtO-Ph	0.00091	<10	53	14	2.5	6.5	30	7.9
57	2-Me-3-pyridyl	3-*n*-PrO-Ph	0.0048	<10	11	7.3	2.9	5.4	67	6.6
58	2-Me-3-pyridyl	3-i-PrO-Ph	0.011	<10	20	6.8	2.7	5.2	51	6.5
59	2-Me-3-pyridyl	3-HCF_2O-Ph	0.027	<10	81	8.4	2.2	5.4	33	6.5

[a] Mean value of at least two experiments. [b] Maximum% activation, maximum concentration = 10 μM. [c] LE fub = pIC_{50} + $\log_{10}$[fub] where fub measured using brain slice method.[34]

Table 5 Selected properties for **41**

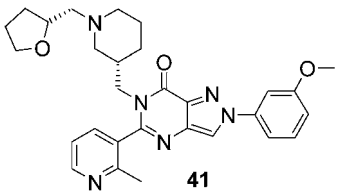

Plasma concn[a] (μM)	1.2
Brain concn[a] (μM)	0.24
Rat brain[b](% free)	8.6
Aq. solubility pH 7.4 (μM)	>1500
h/rat/mu plasma protein binding (% free)	30/42/24

[a] Compound was dosed 20 mg kg^{-1} (mouse), in 1% Pluronic F127 and compound levels measured at 1 h. [b] Measured using brain slice method.[34]

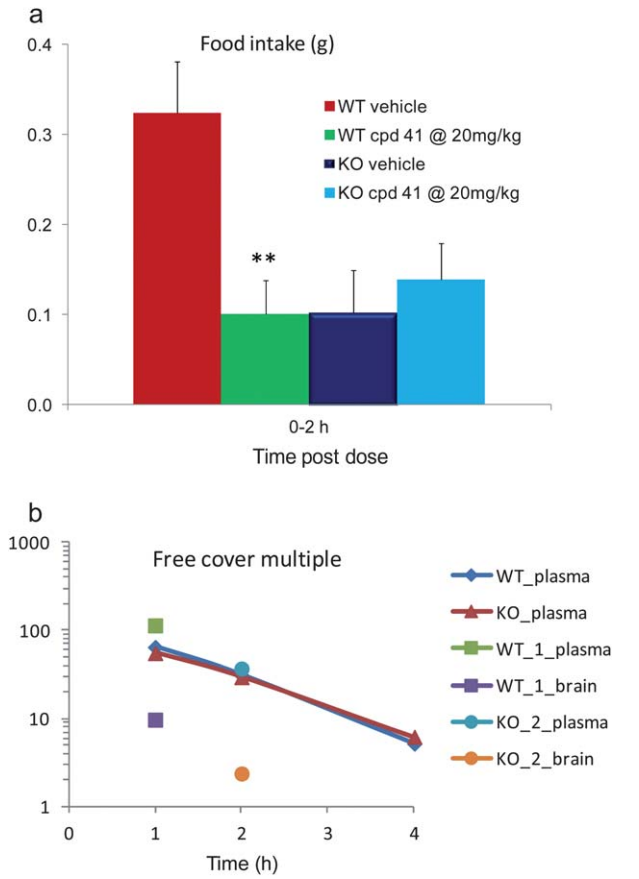

Fig. 3 (a) Pharmacodynamic effect of **41** in GHS-R1a KO and WT mice: food intake (*g*). Mean values ± SEM (**$p < 0.01$). (b) Pharmacokinetic levels of **41** in GHS-R1a KO and WT mice expressed as free cover multiples of binding affinity. 1 and 2 refer to plasma and brain samples taken from the same animal at the same time point of 1 h and 2 h respectively. The 2 h WT_plasma datapoint (blue diamond) is obscured and lies under the 2 h KO_2_plasma time point.

is short lived as during the next time interval (2–4 h), no significant effects on food intake were observed, which is consistent with free exposure levels in brain falling below the binding affinity.

Conclusions

In summary, a scaffold hop from known quinazolinone GHS-R1a antagonists to less lipophilic pyrazolo-pyrimidinones was conducted, followed by further SAR optimization to decrease lipophilicity and reduce hERG activity. Modification of a piperidine substituent was used to convert partial agonists into neutral antagonists and inverse agonists, resulting in **41** which had good overall properties and sufficient oral plasma and CNS exposure for use in preclinical efficacy studies. *In vivo* efficacy of **41** was confirmed in a free feeding study and this effect was shown to be dependent on the expression of GHS-R1a.

Acknowledgements

Teresa Collins, Mark Denn and John Swales are acknowledged for expert technical assistance in generating DMPK data. Dave Masters, Jenny Morrell, Elizabeth Strutynskyj, Steve Bloor, Rob Garcia, Sally Johnson, Susan Aiston and Julie Bartlett's expert technical assistance in generating affinity and functional data is also acknowledged.

Notes and references

1 M. Kojima, H. Hosoda, Y. Date, M. Nakazato, H. Matsuo and K. Kangawa, *Nature*, 1999, **402**, 656–660.
2 M. Kojima, H. Hosoda, H. Matsuo and K. Kangawa, *Trends Endocrinol. Metab.*, 2001, **12**, 118–122.
3 M. W. Schwartz, S. C. Woods, D. Porte Jr, R. J. Seeley and D. G. Baskin, *Nature*, 2000, **404**, 661–671.
4 D. E. Cummings, J. Q. Purnell, R. S. Frayo, K. Schmidova, B. E. Wisse and D. S. Weigle, *Diabetes*, 2001, **50**, 1714–1719.
5 A. M. Wren, L. J. Seal, M. A. Cohen, A. E. Brynes, G. S. Frost, K. G. Murphy, W. S. Dhillo, M. A. Ghatei and S. R. Bloom, *J. Clin. Endocrinol. Metab.*, 2001, **86**, 5992–5995.
6 I. Depoortere, *Regul. Pept.*, 2009, **156**, 13–23.
7 P. A. Carpino and G. Ho, *Expert Opin. Ther. Pat.*, 2008, **18**, 1253–1263.
8 J. Soares, R. Roncon-Albuquerque Jr and A. Leite-Moreira, *Expert Opin. Ther. Targets*, 2008, **12**, 1177–1189.
9 H. Zhao and G. Liu, *Curr. Opin. Drug Discovery Dev.*, 2006, **9**, 509–515.
10 C. Chollet, K. Meyer and A. G. Beck-Sickinger, *J. Pept. Sci.*, 2009, **15**, 711–730.
11 R. S. Ahima, *Endocrinology*, 2007, **148**, 5173–5174.
12 B. Holst and T. W. Schwartz, *Trends Pharmacol. Sci.*, 2004, **25**, 113–117.
13 J. Rudolph, W. P. Esler, S. O'Connor, P. D. G. Coish, P. L. Wickens, M. Brands, D. E. Bierer, B. T. Bloomquist, G. Bondar, L. Chen, C. Chuang, T. H. Claus, Z. Fathi, W. Fu, U. R. Khire, J. A. Kristie, X. Liu, D. B. Lowe, A. C. McClure, M. Michels, A. A. Ortiz, P. D. Ramsden, R. W. Schoenleber, T. E. Shelekhin, A. Vakalopoulos, W. Tang, L. Wang, L. Yi, S. J. Gardell, J. N. Livingston, L. J. Sweet and W. H. Bullock, *J. Med. Chem.*, 2007, **50**, 5202–5216.

14 W. P. Esler, J. Rudolph, T. H. Claus, W. Tang, N. Barucci, S. Brown, W. Bullock, M. Daly, L. DeCarr, Y. Li, L. Milardo, D. Molstad, J. Zhu, S. J. Gardell, J. N. Livingston and L. J. Sweet, *Endocrinology*, 2007, **148**, 5175–5185.

15 J. T. Mihalic, Y. Kim, M. Lizarzaburu, X. Chen, J. Deignan, M. Wanska, M. Yu, J. Fu, X. Chen, A. Zhang, R. Connors, L. Liang, M. Lindstrom, J. Ma, L. Tang, K. Dai and L. Li, *Bioorg. Med. Chem. Lett.*, 2012, **22**, 2046–2051.

16 M. Yu, M. Lizarzaburu, H. Beckmann, R. Connors, K. Dai, K. Haller, C. Li, L. Liang, M. Lindstrom, J. Ma, A. Motani, M. Wanska, A. Zhang, L. Li and J. C. Medina, *Bioorg. Med. Chem. Lett.*, 2010, **20**, 1758–1762.

17 L. Puleo, P. Marini, R. Avallone, M. Zanchet, S. Bandiera, M. Baroni and T. Croci, *Bioorg. Med. Chem.*, 2012, **20**, 5623–5636.

18 P. Hanrahan, J. Bell, G. Bottomley, S. Bradley, P. Clarke, E. Curtis, S. Davis, G. Dawson, J. Horswill, J. Keily, G. Moore, C. Rasamison and J. Bloxham, *Bioorg. Med. Chem. Lett.*, 2012, **22**, 2271–2278.

19 A. Pasternak, S. D. Goble, R. K. deJesus, D. L. Hreniuk, C. C. Chung, M. R. Tota, P. Mazur, S. D. Feighner, A. D. Howard, S. G. Mills and L. Yang, *Bioorg. Med. Chem. Lett.*, 2009, **19**, 6237–6240.

20 F. M. Sabbatini, S. Melotto, G. Bernasconi, S. M. Bromidge, L. D'Adamo, M. Rinaldi, C. Savoia, C. Mundi, C. Di Francesco, L. Zonzini, V. J. A. Costantini, B. Perini, E. Valerio, A. Pozzan, E. Perdonà, F. Visentini, M. Corsi and R. Di Fabio, *ChemMedChem*, 2011, **6**, 1981–1985.

21 M. D. Serby, H. Zhao, B. G. Szczepankiewicz, C. Kosogof, Z. Xin, B. Liu, M. Liu, L. T. J. Nelson, W. Kaszubska, H. D. Falls, V. Schaefer, E. N. Bush, R. Shapiro, B. A. Droz, V. E. Knourek-Segel, T. A. Fey, M. E. Brune, D. W. A. Beno, T. M. Turner, C. A. Collins, P. B. Jacobson, H. L. Sham and G. Liu, *J. Med. Chem.*, 2006, **49**, 2568–2578.

22 D. W. Kung, S. B. Coffey, R. M. Jones, S. Cabral, W. Jiao, M. Fichtner, P. A. Carpino, C. R. Rose, R. F. Hank, M. G. Lopaze, R. Swartz, H. (Tommy) Chen, Z. Hendsch, B. Posner, C. F. Wielis, B. Manning, J. Dubins, I. A. Stock, S. Varma, M. Campbell, D. DeBartola, R. Kosa-Maines, S. J. Steyn and K. F. McClure, *Bioorg. Med. Chem. Lett.*, 2012, **22**, 4281–4287.

23 M. H. Bridgland-Taylor, A. C. Hargreaves, A. Easter, A. Orme, D. C. Henthorn, M. Ding, A. M. Davis, B. G. Small, C. G. Heapy, N. Abi-Gerges, F. Persson, I. Jacobson, M. Sullivan, N. Albertson, T. G. Hammond, E. Sullivan, J.-P. Valentin and C. E. Pollard, *J. Pharmacol. Toxicol. Methods*, 2006, **54**, 189–199.

24 P. D. Leeson and B. Springthorpe, *Nat. Rev. Drug Discovery*, 2007, **6**, 881–890.

25 C. Kusturin, L. S. Liebeskind, H. Rahman, K. Sample, B. Schweitzer, J. Srogl and W. L. Neumann, *Org. Lett.*, 2003, **5**, 4349–4352.

26 K. Yang, X. He, H. Choi, Z. Wang, D. H. Woodmansee and H. Liu, *Tetrahedron Lett.*, 2008, **49**, 1725–1728.

27 J. X. Qiao and P. Y. S. Lam, *Synthesis*, 2011, 829–856.

28 K. Tamura, H. Mizukami, K. Maeda, H. Watanabe and K. Uneyama, *J. Org. Chem.*, 1993, **58**, 32–35.

29 E. Griffen, A. G. Leach, G. R. Robb and D. J. Warner, *J. Med. Chem.*, 2011, **54**, 7739–7750.

30 K. Valko, *J. Chromatogr., A*, 2004, **1037**, 299–310.

31 B. Holst, J. Mokrosinski, M. Lang, E. Brandt, R. Nygaard, T. M. Frimurer, A. G. Beck-Sickinger and T. W. Schwartz, *J. Biol. Chem.*, 2007, **282**, 15799–15811.

32 M. Pilla, M. Andreoli, M. Tessari, S. Delle-Fratte, A. Roth, S. Butler, F. Brown, P. Shah, E. Bettini, P. Cavallini, R. Benedetti, D. Minick, P. Smith, B. Tehan, P. D'Alessandro, O. Lorthioir, C. Ball, V. Garzya, C. Goodacre and S. Watson, *Bioorg. Med. Chem. Lett.*, 2010, **20**, 7521–7524.

33 J. Watson, S. Wright, A. Lucas, K. L. Clarke, J. Viggers, S. Cheetham, P. Jeffrey, R. Porter and K. D. Read, *Drug Metab. Dispos.*, 2009, **37**, 753–760.

34 M. Fridén, F. Ducrozet, B. Middleton, M. Antonsson, U. Bredberg and M. Hammarlund-Udenaes, *Drug Metab. Dispos.*, 2009, **37**, 1226–1233.

